



Contents lists available at ScienceDirect

Journal of Prosthodontic Research

journal homepage: www.elsevier.com/locate/jpor

Original article

Mechanical analysis of the effects of implant position and abutment height on implant-assisted removable partial dentures

Tetsuo Ohyama, DDS, PhD^{a,*}, Shinya Nakabayashi, DDS, PhD^a, Hiroyasu Yasuda, DDS, PhD^a, Takeshi Kase, DDS^b, Shunsuke Namaki, DDS, PhD^c

^a Department of Partial Denture Prosthodontics, Nihon University School of Dentistry, 1-8-13 Kanda-Surugadai, Chiyoda-ku, Tokyo 101-8310, Japan

^b Division of Applied Oral Sciences, Nihon University Graduate School of Dentistry, Tokyo, Japan

^c Department of Clinical Medicine, Nihon University School of Dentistry, Tokyo, Japan

ARTICLE INFO

Article history:

Received 11 June 2019

Revised 18 September 2019

Accepted 25 September 2019

Available online xxx

Keywords:

Implant assisted removable partial denture

IARPD

Implant position

Abutment height

FEM

ABSTRACT

Purpose: An increasing number of clinical reports describe the use of dental implants as abutments in implant-assisted removable partial dentures (IARPD). We used three-dimensional finite element analysis to evaluate IARPD as a unilateral mandibular distal extension denture. Specifically, the mechanical effects of implant position and abutment height on the abutment tooth, denture, and denture-supporting tissue were assessed.

Methods: The models analyzed were defects of the left mandibular second premolar and first and second molars prosthetically treated with an IARPD using one implant for each tooth position. There were two abutment heights: one equal to that of the mucosa and another that was elevated 2 mm above the mucosa. Six models were constructed.

Results: For mucosal-level abutments, movement of the abutment tooth was lower for implants positioned distal to the abutment tooth than for those positioned medial to the abutment tooth. For elevated abutments, movement of the abutment tooth was lower for implants positioned medial to the abutment tooth than for those positioned distal to the abutment tooth.

Conclusions: The mechanical effects on abutment teeth at the same implant position differed in relation to implant abutment height.

© 2019 The Authors. Published by Elsevier Ltd on behalf of Japan Prosthodontic Society.

This is an open access article under the CC BY license. (<http://creativecommons.org/licenses/by/4.0/>)

1. Introduction

An increasing number of reports describe the clinical use of dental implants as abutments in implant-assisted removable partial dentures (IARPD) [1–5]. Because fewer implants are required for the edentulous space, IARPD are less invasive and cheaper than fixed implant bridges [3,4]. In addition, IARPD minimize denture movement because they enhance implant support and diversify the fulcrum line [1–5]. Previous studies reported that increased implant support decreased denture movement [6–8]; however, few studies have used finite element analysis to examine IARPD effectiveness with respect to mechanical characteristics. In particular, the biomechanical effects of implant position and the bracing effect on tissues surrounding the implant in free-end dentures are not well understood.

In this study, we used three-dimensional finite element analysis to evaluate prosthetic treatment with IARPD as a unilateral mandibular distal extension denture. Specifically, to clarify criteria for selection of implant position and optimal abutment height in patients requiring IARPD, we assessed the mechanical effects of implant position and abutment height on abutment teeth, dentures, and denture-supporting tissue.

2. Materials and methods

2.1. Analytic models

Defects in left mandibular second premolars and first and second molars were analyzed in models of prosthetic treatment with IARPD using one implant (Fig. 1). The components of the analytic model were the teeth (dentin), cancellous bone, cortical bone, mucosa, periodontal ligament, metal crown, denture base, metal flange, implant, and abutment. One implant was positioned at the site of the second premolar or first or second molar. Six models were analyzed: three (5-0, 6-0, 7-0) used mucosal-level abutments

* Corresponding author.

E-mail address: ohyama.tetsuo@nihon-u.ac.jp (T. Ohyama).

<https://doi.org/10.1016/j.jpor.2019.09.007>

1883-1958/© 2019 The Authors. Published by Elsevier Ltd on behalf of Japan Prosthodontic Society. This is an open access article under the CC BY license. (<http://creativecommons.org/licenses/by/4.0/>)

Table 1
Properties of materials used.

Model	Young's modulus (MPa)	Poisson's ratio
Teeth (dentin)	1.37×10^4	0.3
Cancellous bone	7.80×10^3	0.3
Cortical bone	2.28×10^4	0.3
Mucosa	4.50×10^{-2}	0.49
Periodontal ligament (1st load)	4.90×10^{-2}	0.49
Periodontal ligament (2nd load)	0.30×10^1	0.49
Metal crown (gold-silver-palladium alloy)	8.13×10^4	0.3
Denture base (acrylic resin)	2.38×10^3	0.3
Flame work (Co-Cr alloy)	2.18×10^5	0.3
Implant, abutment (titanium)	1.17×10^5	0.3

The properties of the periodontal ligament and mucosa approximate previously reported pressure-displacement values. To reproduce biphasic tooth movement, two types of periodontal ligament (with differing properties) were used.

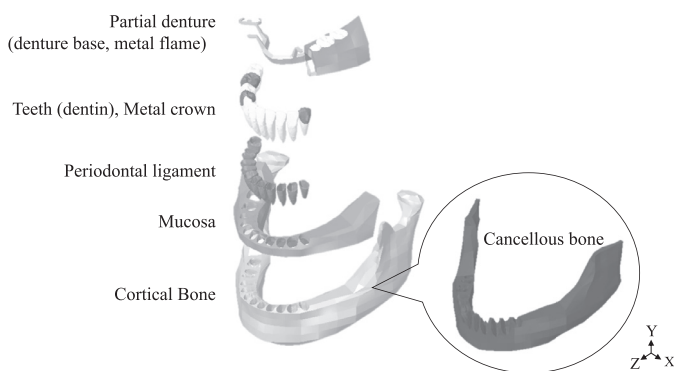


Fig. 1. Analytic model (Base model). The analytic model comprised defects of the left mandibular second premolar and first and second molars, which were prosthodontically treated with IARPD. The implant is not positioned in this basic model.

(ML abutments) and three (5-2, 6-2, 7-2) used abutments 2 mm higher than the mucosal-level abutments (H abutments) (Fig. 2). The analytic model was constructed by processing computed tomography (Asteion Super 4 Edition, Toshiba, Tokyo, Japan) images of a skull replicative model (P10-SB1, Nissin, Kyoto, Japan) with CAD software (Rhinoceros Ver 1.0, Robert McNeel & Associates, Seattle, WA, USA), 3D direct modeler (Space Claim Direct Modeler, Space Claim Co., Canonsburg, PA, USA), and finite element software (ANSYS Rel. 18.2, ANSYS Inc., Canonsburg, PA, USA). Cortical bone, cancellous bone, and mucosa were modeled in accordance with previously reported data [9–11].

A screw-type implant was used (platform diameter, 4.1 mm; implant diameter, 3.75 mm; length, 10.0 mm with reference to the Brånemark System; MKIII RP, Nobel Biocare Services AG, Zurich, Switzerland). The implant was placed perpendicularly to the tentative occlusal plane. The central axes of the implant and abutment were aligned, and the implant platform height was set to correspond with the top of the cortical bone. The bone contact rate between the implant and cortical bone was 100%. The framework design for the retainer was an RPI clasp for the left first premolar, a mesial rest for the right primary premolar, and an Akers clasp for the right first molar; the major connector was a lingual bar. A rectangular coordinate system was used, where the XY plane is the frontal plane, the YZ plane is the sagittal plane, and the XZ plane is the horizontal plane. The occlusal plane was parallel to the XZ plane.

2.2. Material properties

The properties of the materials are shown in Table 1 [12–21]. The material properties of the periodontal ligament and mu-

cosa approximate previously reported pressure-displacement values [12,14,16]. To reproduce biphasic movement of teeth, two different types of periodontal ligament were used.

2.3. Loading and boundary conditions

Loading and boundary conditions are constrained by occlusal contact and loading of the mandible by masticatory muscles during biting in the intercuspal position, that is, the load defines muscle activity as a contraction vector of each muscle [22]. The involved muscles are the masseter muscles (shallow and deep), medial pterygoid muscles, temporalis muscles (anterior, middle, and posterior), lateral pterygoid muscles (upper and lower), and the anterior belly of the digastric muscles (Fig. 3, Table 2) [22].

2.4. Analysis

Mechanical analysis was done by using isotropic structural nonlinear static analysis, with finite element analysis software (ANSYS Mechanical Rel.18.2 ANSYS, Inc., Canonsburg, USA). Contact elements that reproduced discontinuities between model components were also used between the denture base and mucosa, between the metal frame and teeth, between two teeth, and between the denture base and abutment. The analytic models were tetrahedral meshes constructed with the mesh tool in the ANSYS software program. The models comprised 278,792 elements and 506,036 nodes for the 5-0 model, 278,654 elements and 505,986 nodes for the 6-0 model, 277,007 elements and 503,768 nodes for the 7-0 model, 279,283 elements and 507,106 nodes for the 5-2 model, 280,492 elements and 509,088 nodes for the 6-2 model, and 280,144 elements and 508,162 nodes for the 7-2 model.

2.5. Variables evaluated

The variables evaluated were displacement of the left mandibular first premolar and denture base and minimum principal stress of the cortical bone around the implant neck. The distance and direction of displacement of the right mandibular first premolar and denture base were measured in relation to the cortical bone of the tooth and denture base. The measurement points for the right mandibular first premolar were the tip of the buccal cusp and root apex (Fig. 4). In addition, 16 points on the inner surface of the denture base were analyzed (Fig. 4). Stress on cortical bone around the implant was evaluated by using contour images of minimum principal stress distribution and minimum principal stress values.

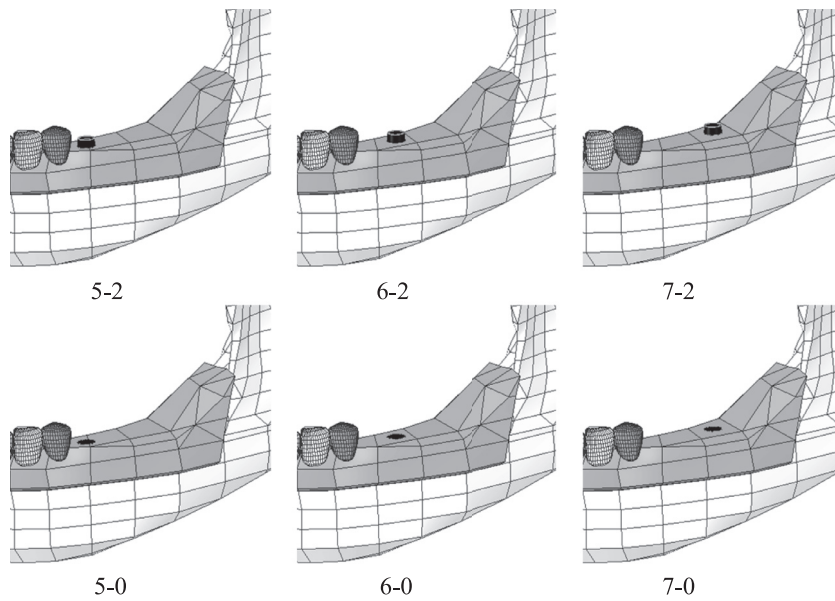


Fig. 2. Analytic model (implant-positioned model). The implant was positioned at the site of the second premolar or first or second molar. Six models were constructed: three (5-0, 6-0, 7-0) with the abutment at the height of the mucosa and three with the abutment extending 2 mm above the mucosa (5-2, 6-2, 7-2).

Table 2
Loading force.

		Node numbers	Loading force (N)
Masseter muscle	Shallow part	14	190.4
	Deep part	5	81.6
Medial pterygoid muscle		11	132.8
Temporal muscle	Anterior part	9	154.8
	Middle part	12	91.8
	Posterior part	9	72.6
Lateral pterygoid muscle	Superior head	3	16.9
	Inferior head	3	18.1
Digastric muscle	Anterior belly	1	11.2

Mechanical analysis at the intercuspal position was possible because, by constraining the occlusal contact point and loading the putative muscles of the mandible, the models were able to closely simulate the forces in the human body.

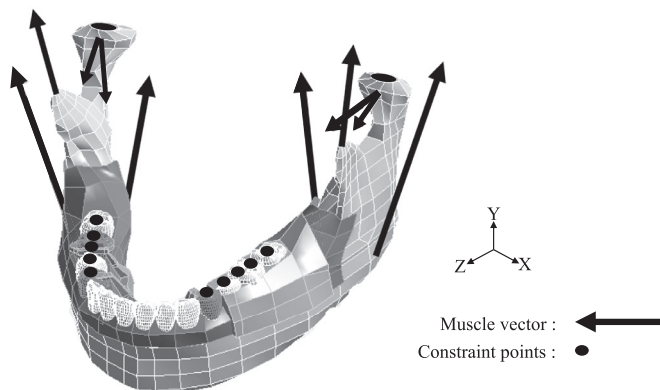


Fig. 3. Loading and boundary conditions. Loading and boundary conditions were constrained by occlusal contact and loading of the mandible by masticatory muscles during biting in the intercuspal position. The muscles involved are the masseter muscles (shallow, deep), medial pterygoid muscles, temporalis muscles (anterior, middle, posterior), lateral pterygoid muscles (upper, lower), and the anterior belly of the digastric muscles.

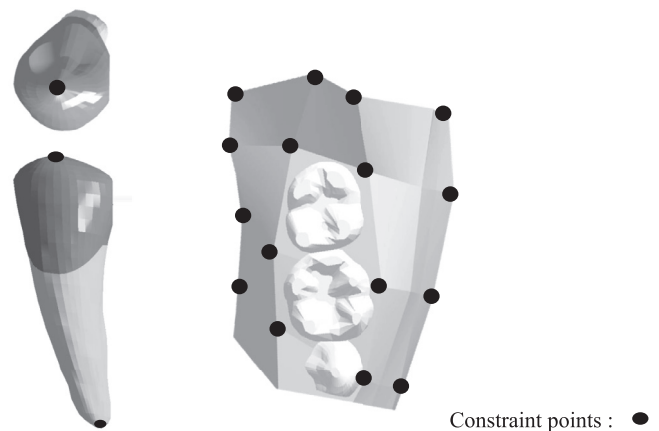


Fig. 4. Measurement points. The measurement points were the tip of the buccal cusp and root apex of the right mandibular first premolar and 16 points on the inner surface of the denture base.

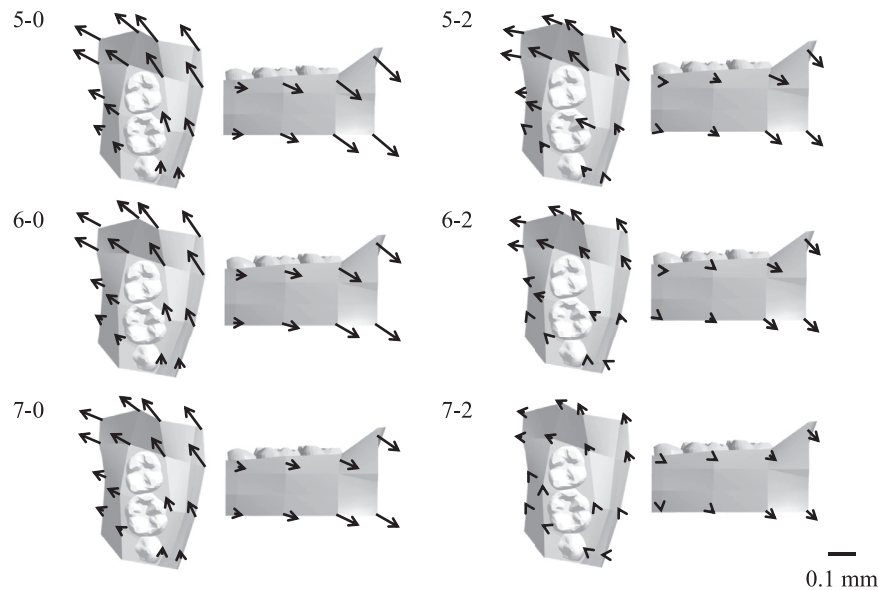


Fig. 5. Displacement and direction vectors. The displacement and direction vectors for each measurement point are shown in occlusal and labial views of the denture base.

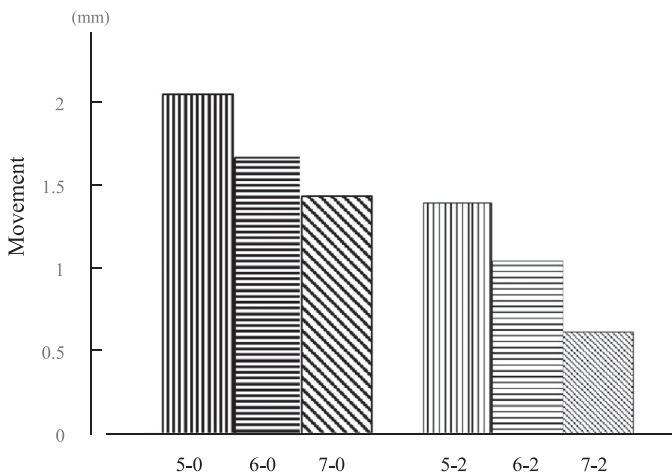


Fig. 6. Displacement distance of denture base. The graph shows the sums of the displacement distances at the measurement points of the denture base.

3. Results

3.1. Displacement

3.1.1. Denture base

The displacement and direction vector for each measurement point in occlusal and labial views of the denture base are shown in Fig. 5. The sums of the displacement distances at the measurement points in the denture base are shown in Fig. 6. Distolingual subsidence of the denture base was observed in all models (Fig. 5). Displacement was greater for H abutments (5-2, 6-2, 7-2) than for ML abutments (5-0, 6-0, 7-0) (Fig. 6).

3.1.2. Abutment teeth

Fig. 7 shows vector graphical occlusal and buccal views of the tip of the buccal cusp and root apex. The sums of the displacement distances at the tip of the buccal cusp and root apex of the left mandibular first premolar are shown in Fig. 8. Tooth axes were markedly distally inclined in models 5-2, 6-2, and 7-2 and slightly buccally inclined in models 5-0, 6-0, and 7-0 (Fig. 7). Displacement

distance was lower for models 5-2, 6-2, and 7-2 than for models 5-0, 6-0, and 7-0 (Fig. 8). In models 5-0, 6-0, and 7-0, displacement was lower when the implant was placed in the distal position; however, in models 5-2, 6-2, and 7-2, displacement was greater when the implant was placed in the distal position (Fig. 8).

3.2. Minimum principal stress

Fig. 9 shows contour images of minimum principal stress in cortical bone. Minimum principal stress values were originally calculated as negative numbers but are presented as positive numbers (in MPa) in the images, after simple positive–negative conversion. Maximum minimum principal stress values in cortical bone are shown in Fig. 10. In all models, minimum principal stress was concentrated at the distal point of the implant neck (Fig. 9). Stress was greater and more widely distributed in models 5-2, 6-2, and 7-2 than in models 5-0, 6-0, and 7-0 (Fig. 9). Minimum principal stress values were higher for models 5-2, 6-2, and 7-2 than for models 5-0, 6-0, and 7-0 (Fig. 10). In models 5-0, 6-0, and 7-0, minimum principal stress values were higher when the implant was located distally; however, in models 5-2, 6-2, and 7-2, minimum principal stress values were lower when the implant was located distally (Fig. 10).

4. Discussion

4.1. Analysis models

This study did not use conventional partial dentures without implants as negative controls, because previous clinical reports [1–5] and analyses of mechanics [6–8] reported that denture movement was more limited for partial implant overdentures than for conventional partial dentures. We therefore chose to investigate implant position and the height of the implant abutment.

In biomechanical analysis using finite element analysis, the extent of the similarity between the analytical model and human body greatly affects reliability. In dental research, many mechanical studies that use finite element analysis utilize constraints at the lower part of the analytic model and loads from the direction of the occlusal surface [6–8]. However, during occlusal contact—as the mandible is pulled up by multiple muscles—occlusal force acts

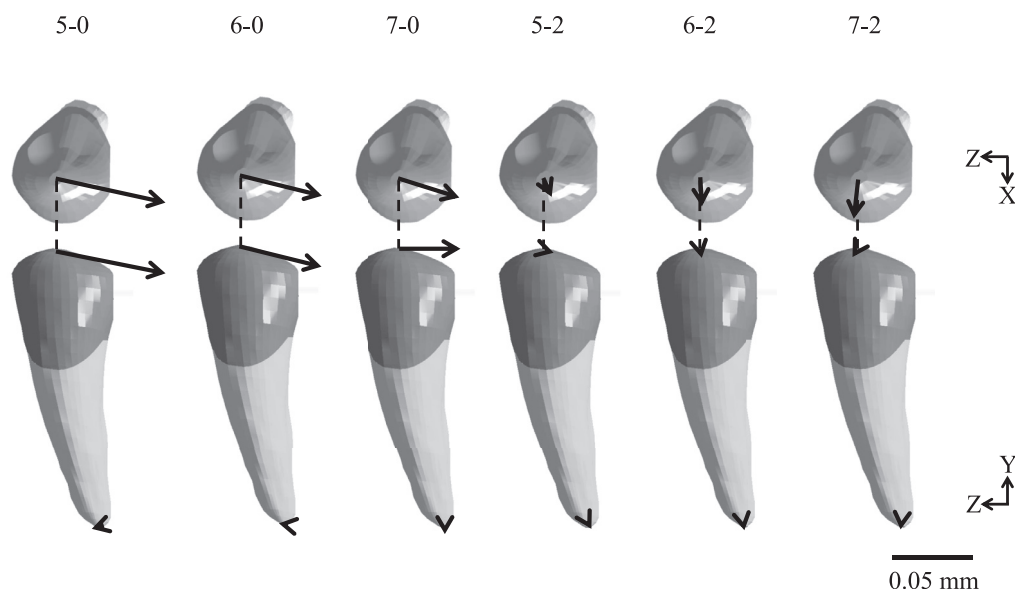


Fig. 7. Displacement and direction vectors for left mandibular first premolars. The figure shows occlusal and buccal vector graphical images of the tip of the buccal cusp and root apex.

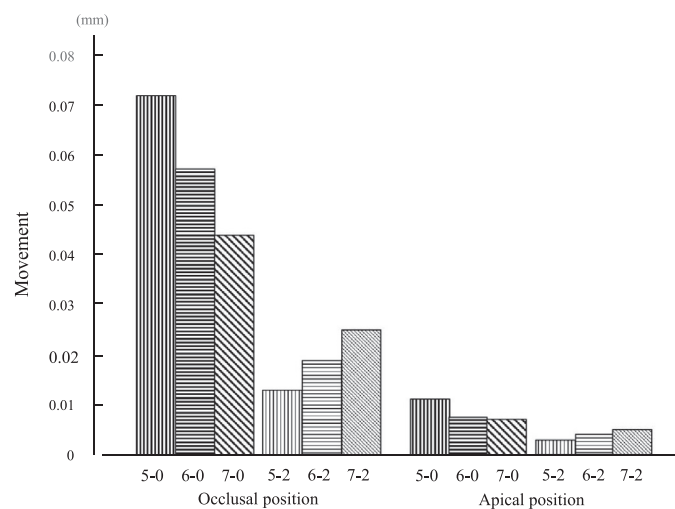


Fig. 8. Displacement distance for the left mandibular first premolar. The graph shows the sum of displacement distances at the tip of the buccal cusp and root apex of the left mandibular first premolar.

on the tooth. In this study, mechanical analysis at the intercuspal position was possible because, by constraining the occlusal contact point and loading the putative muscles of the mandible, the models were able to closely simulate the forces in the human body [19].

4.2. Denture movement

In IARPD, the morphology of the implant abutment affects denture movement. In particular, H abutments exhibited no change in the direction of denture movement, which was not the case for ML abutments with the same implant positions; however, the distance of denture movement was lower. This finding is likely attributable to suppression of denture movement in the sinking direction, regardless of the height of the implant abutment. In contrast, H abutments were associated with less horizontal movement. In addition, positioning the implant distal to the tooth abutment reduced denture movement, regardless of abutment height, perhaps because an

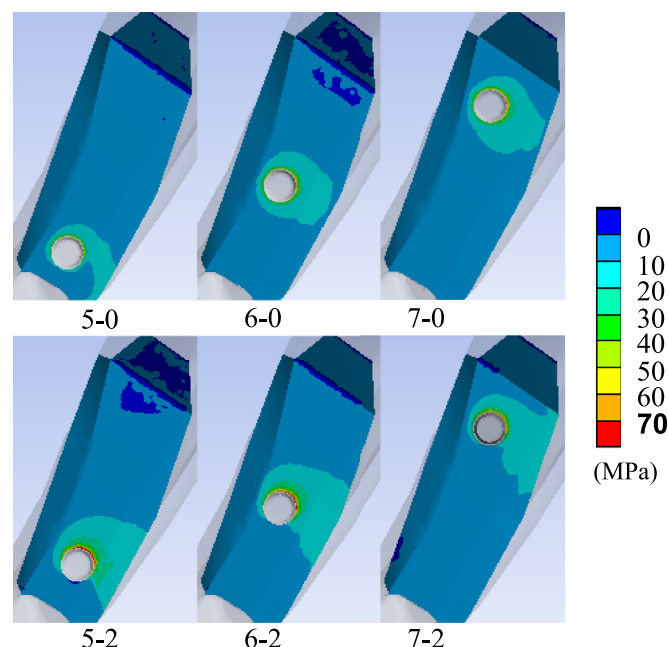


Fig. 9. Contour images of minimum principal stress in cortical bone. Values for minimum principal stress were originally calculated as negative numbers but are presented as positive numbers (in MPa), after simple positive-negative conversion.

increase in the distance between the abutment teeth and implant improves the stability of dental prostheses.

4.3. Movement of abutment teeth

In IARPD, the morphology of the implant abutment affects movement of the abutment tooth. In particular, abutment movement was lower for H abutments than for ML abutments, for the same implant position. For ML abutments, abutment teeth moved less when the implant was positioned distal to the abutment tooth than when it was positioned medial to the abutment tooth. However, for H abutments, abutment teeth moved less when the implant was positioned medial to the abutment tooth. In ML abut-

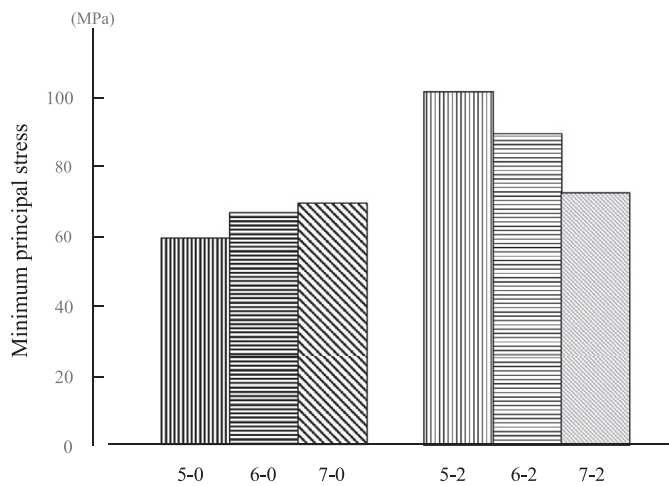


Fig. 10. Minimum principal stress. The graph shows maximum values for minimum principal stress in cortical bone. Values for minimum principal stress were originally calculated as negative numbers but are presented as positive numbers (in MPa), after simple positive-negative conversion.

ments, abutment tooth movement was synchronized with denture movement. However, in H abutments, movement of abutment teeth was better suppressed by bracing when the implant abutment and abutment teeth were closer. Positioning an implant close to the abutment tooth is aesthetically desirable, as a retention arm does not need to be applied to the abutment tooth [23]. However, the present results suggest that, with respect to bracing by the abutment of an implant, the implant should be placed close to the abutment tooth, as this is aesthetically preferable and protects the abutment tooth.

4.4. Minimum principal stress on the implant neck

The minimum principal stress distribution around the implant neck changed in relation to the morphology of the abutment of the implant in IARPD. Minimum principal stress values at the implant neck were lower for H abutments than for ML abutments, for the same implant positions. Minimum principal stress values for distal implants were lower for H abutments than for ML abutments (Fig. 10), because the bracing effect of higher abutments directly suppressed abutment tooth movement. In addition, minimum principal stress was higher when the implant was closer to the abutment tooth, and more affected by abutment movement, than when it was located distally.

5. Conclusion

When using IARPD for prosthetic mandibular unilateral distal extension, implant abutment morphology affects the movement of the denture and abutment tooth and the distribution of minimum principal stress on cortical bone near the implant neck.

Denture movement was more limited for higher abutments than for mucosal-level abutments, for implants at the same position. For mucosal-level abutments, movement of the abutment tooth was less for implants distal to the abutment tooth than for those medial to the abutment tooth. The mechanical effects on abutment teeth at the same implant position differed in relation to implant abutment height.

Abutment tooth movement was more limited when implants were positioned medial to abutment teeth than when they were positioned distal to abutment teeth.

Finally, minimum principal stress values were lower when the implant neck was located distally.

Declaration of Competing Interest

The authors have no conflicts of interest that are directly relevant to the content of this article.

Acknowledgments

This research was supported by a grant from the Dental Research Center of Nihon University School of Dentistry.

Reference

- [1] Giffin KM. Solving the distal extension removable partial denture base movement dilemma: a clinical report. *J Prosthet Dent* 1996;76:347–9.
- [2] Halterman SM, Rivers JA, Keith JD, Nelson DR. Implant support for removable partial overdentures a case report. *Implant Dent* 1998;8:74–8.
- [3] Kuzmanovic DV, Payne AG, Purton DG. Distal implant to modify the Kennedy classification of a removable partial denture: a clinical report. *J Prosthet Dent* 2004;92:8–11.
- [4] Ramchandran A, Agrawal KK, Chand P, Ramashanker, Singh RD, Gupta A. Implant-assisted removable partial denture: an approach to switch Kennedy class 1 to Kennedy class III. *J Indian Prosthodont Soc* 2016;16:408–11.
- [5] Bural C, Buzbas B, Ozatik S, Bayraktar G, Emes Y. Distal extension mandibular removable partial denture with implant support. *Eur J Dent* 2016;10:566–70.
- [6] Verri FR, Pellizzer EP, Rocha EP, Pereira JA. Influence of length and diameter of implant associated with distal extension removable partial denture. *Implant Dent* 2007;16:270–80.
- [7] Memari Y, Geramy A, Fayaz A, Rezvani Habib Abadi S, Mansouri Y. Influence of implant position on stress distribution in implant-assisted distal extension removable partial dentures: a 3D finite element analysis. *J Dent(Tehran)* 2014;11:523–30.
- [8] Ortiz-Puigpelat O, Lázaro-Abdulkarim A, de Medrano-Reñé JM, Gargallo-Albiol J, Cabratosa-Termes J, Hernández-Alfaro F. Influence of implant position in implant-assisted removable partial denture: a three-dimensional finite element analysis. *J Prosthodont* 2019;28:e675–81.
- [9] Dong J, Zhang FY, Wu GH, Zhang W, Yin J. Measurement of Mucosal Thickness in Denture-bearing Area of Edentulous Mandible. *Chinese Medical J* 2015;128:342–7.
- [10] Promma L, Sakulsak N, Putiwat P, Amarttayakong P, Iamsaard S, Trakulsuk H, et al. Cortical bone thickness of the mandibular canal and implications for bilateral sagittal split osteotomy: a cadaveric study. *Int J Oral Maxillofac Surg* 2017;46:572–7.
- [11] Nucera R, Lo Gludice A, Bellocchio AM, Spinuzza P, Caprioglio A, Perillo L, et al. Bone and cortical bone thickness of mandibular buccal shelf for mini-screw insertion in adults. *Angle Orthod* 2017;87:745–51.
- [12] Muhlemann HR. Periodontometry, a method for measuring tooth mobility. *Oral Surg Oral Med Oral Pathol* 1951;4:1220–33.
- [13] Stanford JW, Weigel KV, Paffenbarger GC, Sweeney WT. Compressive properties of hard tooth tissues and some restorative materials. *J Am Dent Assoc* 1960;60:746–56.
- [14] Parfitt GJ. Measurement of the physiological mobility of individual teeth in an axial direction. *J Dent Res* 1960;39:608–18.
- [15] Morris HF, Asgar K. Physical properties and microstructure of four new commercial partial denture alloys. *J Prosthet Dent* 1975;33:36–46.
- [16] Wills DJ, Manderson RD. Biomechanical aspects of the support of partial dentures. *J Dent* 1977;5:310–18.
- [17] Mente PL, Lewis JL. Experimental method for the measurement of the elastic modulus of trabecular bone tissue. *J Orthop Res* 1989;7:456–61.
- [18] Caycik S, Jagger RG. The effect of cross-linking chain length on mechanical properties of a dough-molded poly (methylmethacrylate) resin. *Dent Mater* 1992;8:153–7.
- [19] Niinomi M. Mechanical properties of biomedical titanium alloys. *Mater Sci Eng* 1998;A243:231–6.
- [20] Goto S, Nakai A, Miyagawa Y, Ogura H. Development of Ag-Pd-Au-Cu alloys for multiple dental applications Part2 Mechanical properties of experimental Ag-Pd-Au-Cu alloys containing Sn or Ga for ceramic-metal restorations. *Dent Mater J* 2001;20:135–47.
- [21] Schwartz-Dabney CL, Dechow PC. Variations in cortical material properties throughout the human dentate mandible. *Am J Phys Anthropol* 2003;120:252–77.
- [22] Koriath TW, Hannam AG. Deformation of the human mandible during simulated tooth clenching. *J Dent Res* 1994;73:56–66.
- [23] Grossmann Y, Nissan J, Levin L. Clinical effectiveness of implant-supported removable partial dentures: a review of the literature and retrospective case evaluation. *J Oral Maxillofac Surg* 2009;67:1941–6.